A Dynamic population of prophase CENP-C is required for meiotic chromosome segregation

Jessica E. Fellmeth, Hannah Sturm, Janet Jang, Neha Changela, Aashka Parikh, Manisha Persaud and Kim S. McKim

Waksman Institute and Department of Genetics, Rutgers, the State University of New Jersey, Piscataway, New Jersey, United States of America.

Correspondence: Kim S. McKim (mckim@waksman.rutgers.edu)

Corresponding author: Kim S. McKim

190 Frelinghuysen Road,

Piscataway, NJ-08854

848-445-1164

mckim@waksman.rutgers.edu

Summary

The centromere is an epigenetic mark that is a loading site for the kinetochore during meiosis and mitosis. This mark is characterized by the H3 variant CENP-A, known as CID in *Drosophila*, which replaces canonical H3 at the centromeres. In *Drosophila*, CENP-C is critical for maintaining CID at the centromeres and directly recruits outer kinetochore proteins after nuclear envelope break down. It is not clear, however, if these two functions require the same population of CENP-C. In *Drosophila* and many other metazoan oocytes, centromere maintenance and kinetochore assembly are separated by an extended prophase. We used RNAi knockdown, mutants, and transgenes to study the dynamics and function of CENP-C in meiosis. CENP-C that is incorporated into cells prior to the onset of meiosis is involved in centromere maintenance and CID recruitment. We found this is not sufficient for the other functions of CENP-C. Indeed, CENP-C is loaded during meiotic prophase, while CID and the chaperone CAL1 are not. CENP-C prophase loading is required for meiotic functions at two different times. In early meiotic prophase, CENP-C loading is required for sister centromere cohesion and centromere clustering. In late meiotic prophase, CENP-C loading is required to recruit kinetochore proteins. Thus, CENP-C is one of the few proteins that links the function of the centromeres and kinetochores through the long prophase pause in oocytes.

INTRODUCTION:

The chromatin of the centromere is characterized by an H3 variant known as CENP-A rather than a specific sequence [1, 2]. One of its main functions is to recruit kinetochore proteins for meiosis and mitosis [3]. Failure to maintain the centromere after DNA replication or failure to recruit an effective kinetochore during M-phase can result in chromosome segregation defects, which is a feature of many cancers, infertility, and developmental disorders. In *Drosophila*, CENP-A is encoded by the *cid* gene [4].

CENP-A interacts with the “constitutive centromere associated network” (CCAN) complex in a wide variety of organisms such as humans and yeast [3]. The CCAN contains many proteins that form multiple links between the inner centromere and the outer kinetochore. In many vertebrate cells, two pathways defined by the components CENP-T and CENP-C provide the link between the centromere and outer kinetochore [5]. In some cases, one of these pathways has been lost during evolution. *C. elegans* and *Drosophila* are examples where most or all CCAN proteins have been lost and CENP-C forms the only linkage between the inner centromere and outer kinetochore.

Centromeres are maintained by loading new CENP-A once per cell cycle, but unlike other centromeric histones, this does not occur during S-phase. Thus, CENP-A levels are reduced during S-phase and return to normal levels once during the cell cycle. The timing of CENP-A loading varies in different species and possibly cell types, but typically occurs once per cell cycle, usually during M or G1 [6-8]. In yeast and mammals, maintenance of centromeric CENP-A depends on CENP-C, the Mis18 complex, and HJURP [9-15]. In *Drosophila*, the Mis18 complex and HJURP are absent, but CAL1 takes on a similar role by interacting with both CENP-C and CID [16-18]. CID,

CENP-C, and CAL1 rely on each other for loading to maintain centromere identity [10, 16, 18, 19].

While CENP-C is required for centromere maintenance, it also has a direct role in kinetochore assembly by recruiting MIS12 in mammals [20-22] and *Drosophila* [23-25]. In many organisms, including *Drosophila* and mammals, the kinetochore is loaded once the nuclear envelope breaks down, and is only present during cell division. Although considered part of the inner kinetochore, CENP-C is present throughout the cell cycle. In *Drosophila,* no other kinetochore proteins except for MIS12 exhibit this behavior [26]. CENP-C recruits MIS12 [24, 25], and they directly interact to form an inner kinetochore complex that is present throughout the cell cycle [21, 23, 27].

Following the pachytene stage of meiosis, mammalian and *Drosophila* oocytes enter a long pause in prophase. If centromere proteins are loaded once per cell cycle, they would have to be maintained for a long time before kinetochores are assembled and cell division commences [28]. Cohesins, for example, are loaded during S-phase and deteriorate with age, causing aneuploidy in older mothers [29, 30]. However, CENP-A nucleosomes in the mouse are stable and do not need to be maintained during meiotic prophase [28]. Furthermore, CENP-C becomes immobilized at metaphase [31]. Thus, it is possible that the CENP-C loaded along with CENP-A in G1 is sufficient for kinetochore assembly. However, the stability of CENP-C during meiotic prophase has not been tested. How age affects proteins like CENP-C that are loaded before or during the prophase pause is poorly understood and important for oocytes health [32].

In this study, we investigated the meiotic prophase dynamics of CENP-C, CAL1, and CID. As with CENP-A in mouse oocytes [28], we found that CID is stable

94 throughout *Drosophila* oocyte meiotic prophase, and there was little addition of new
95 subunits. CAL1 is gradually lost during prophase and is absent in metaphase I oocytes.
96 CENP-C is uniquely loaded at centromeres using an exchange mechanism during
97 prophase, and this is required for assembly of the meiotic kinetochore. Thus, CENP-C is
98 loaded independently of centromere maintenance in a process that is required for
99 kinetochore assembly.
100

RESULTS

CENP-C, but not CAL1 or CID, loads onto centromeres during prophase I

The analysis of centromere protein dynamics during prophase is facilitated by the organization of the *Drosophila* ovary. Each of *Drosophila's* two ovaries contains several strings, or ovarioles, of developing oocytes (Figure 1A). At the anterior end of each ovariole is the germarium, which includes mitotically dividing cells (region 1) and early meiotic prophase (regions 2-3). Region 3 (stage 1) oocytes leave the germarium and enter the vitellarium. During stages 1-12, meiosis remains in prophase while the oocyte grows and matures. At the posterior end of the ovariole (stage 13-14), the oocyte enters prometaphase. Meiosis arrests at metaphase I until passage through the oviduct and fertilization occurs.

The dynamics of CENP-C during meiotic prophase was investigated along with comparisons to its known centromeric partners, CAL1 and CID. Expression of *UASP* regulated EGFP-tagged transgenes of *Cenp-C, cal1,* and *cid* were induced during female meiotic prophase by crossing to one of three GAL4-expressing strains (Figure 1). *P{GAL4: :VP16-nos.UTR}CG6325*^{MVD1} (referred to as *MVD1*) initiates expression of transgenes in the pre-meiotic cyst cells of the germline and continues throughout oocyte maturation [33]. *P{GAL4-nos.NGT}A* (referred to as *NGTA*) expresses only during early prophase (Figure S 1). *P{w[+mC]=matalpha4-GAL-VP16}V37* (referred to as *mata*) expression begins late in prophase (region 2B/3) and continues through metaphase I in the stage 14 oocyte [34, 35]. We expressed the EGFP-tagged transgenes using one of these promoters to determine whether centromeric loading of each protein could occur during prophase.

Experiments with *MVD1* showed CID, CAL1, and CENP-C localization in region 2a and throughout stages 1 to 5 of oogenesis (Figure 1B-D). These results may closely resemble wild-type expression because *MVD1* promotes expression of UAS transgenes through all stages of the germline. We also observed centromeric localization of EGFP-tagged CID, CAL1, and CENP-C in region 2a and stages 1-5 when expressed with *NGTA*. This is consistent with expression of *NGTA* in the early stages of the germarium, including the mitotic divisions. Similar results were observed using an *HA-Cenp-C* transgene with *NGTA* (Figure S 2A).

We did not observe centromeric localization of EGFP-tagged CID or CAL1 when expressed during late prophase I using *mata* (Figure 1B, C). In contrast, centromeric localization of CENP-C was observed in late prophase when expressed with *mata* (Figure 1D, Figure S 2A,B). These data indicate that meiotic CENP-C dynamics are different than CID and CAL1. CENP-C is loaded onto the centromeres during meiotic prophase. In addition, heat shock was used to induce expression of *Cenp-C*, which also showed evidence of prophase loading of CENP-C (Figure S 2C). Together, these results suggest a prophase function for CENP-C that is independent of centromere establishment or maintenance.

While EGFP-CENP-C under the control of *NGTA* resulted in centromeric GFP localization in stages 1-5 (see above), it was absent in stage 14 oocytes (Figure 1D). These results suggest that CENP-C is unloaded from the centromeres during meiotic prophase. In contrast, CID was retained at the centromeres in stage 14 when expressed using *NGTA* (Figure 1B), suggesting CID loaded prior to meiotic prophase is maintained throughout late prophase of oogenesis. Surprisingly, CAL1 showed a different pattern

with *NGTA* and *MVD1*. CAL1 localized in early prophase oocytes similarly to CID but was not detected in stage 14 oocytes (Figure 1C, Figure S 3). Thus, like CENP-C, CAL1 is unloaded during prophase, but unlike CENP-C, CAL1 is not loaded during this time.

CENP-C regulates centromere clustering, recombination, and MIS12 loading in early prophase I

These results show there is a population of CENP-C loaded during meiotic prophase that is distinct from the population required for the maintenance of CID at the centromeres. To investigate *Cenp*-C function in early prophase, we knocked down the expression by RNAi using an shRNA (*GL00409*) and the *NGTA* or *MVD1* promoters. Females expressing *GL00409* with *MVD1* (*GL00409*/*MVD1* oocytes) were sterile and agametic. *MVD1* expression initiates early in the primordial germ cells of the embryo and a requirement for CENP-C during these mitotic divisions would explain the agametic phenotype. Thus, the remaining early prophase experiments were performed with females expressing *GL00409* with *NGTA* (*GL00409/NGTA* oocytes).

GL00409/NGTA females were fertile but displayed a high level of homologous chromosome nondisjunction (7%) compared to controls (0.25%) (Table 1). A similar result was observed with a different shRNA (*HMJ21500*). *NGTA* expression peaks during early prophase, affecting *Cenp-C* expression for only a limited time. Therefore, these results suggest CENP-C has an early meiotic function required for chromosome segregation that is separable from centromere maintenance. To investigate the mechanisms of nondisjunction caused by loss of CENP-C, we characterized processes

that occur early in meiotic prophase such as centromere assembly, meiotic recombination, centromere pairing and synaptonemal complex (SC) formation.

The intensity CENP-C or CID at the centromeres was not significantly decreased in early prophase nuclei of *GL00409*/*NGTA* oocytes (Figure 2A - C). The absence of a reduction in CID suggests that inhibition of CENP-C occurred after CID was loaded and did not affect centromere maintenance. The failure to observe a significant reduction in CENP-C may have been due to the abundance of protein required for CID maintenance. For another measure of CENP-C function in prophase, we examined MIS12. In mitotic cells, CENP-C promotes kinetochore assembly by recruiting MIS12 [23]. MIS12-GFP localization was observed in the same prophase stages as CENP-C in control oocytes, starting in region 2a of the germarium (Figure 2D). The intensity of centromeric MIS12-GFP was significantly reduced in *GL00409/NGTA* females (Figure 2D, E) indicating that CENP-C promotes recruitment of MIS12 during meiotic prophase. These results show that MIS12 localizes to the centromeres in meiotic prophase and depends on CENP-C.

Increased frequencies of nondisjunction can be associated with loss of SC and/or a reduction in crossing over (CO) [36]. SC assembly in *GL00409/NGTA* females was found to be normal, indicated by the thread-like appearance of transverse filament protein C(3)G [37] (Figure S 4). We genetically measured the frequency of COs in *GL00409/NGTA* females and observed an increase in centromeric crossovers, but overall, crossing over was not decreased (Table 1). In a separate experiment where the centromeres were genetically marked (see Methods), we observed an increase in sister

chromatid nondisjunction. Thus, the meiotic nondisjunction may be occurring because of loss of cohesion rather than crossing over.

A cohesion defect can be observed as an increase in the number of centromere foci [38, 39]. Indeed, there was an increased number of CID foci in the germaria of *GL00409/NGTA* ovaries, indicating a separation of centromeres (Figure 2F, G). However, nonhomologous centromeres normally cluster in early prophase. Therefore, we used chromosome-specific FISH probes for the pericentromeric regions of the X, 2nd, and 3rd chromosomes to examine pairing of the centromeres in early prophase of *GL00409/NGTA* oocytes. Clustering defects were defined as nuclei containing 3 or more clearly separated probe foci (of any color) where control oocytes had 1-2 foci. Pairing defects were defined as greater than one nuclear focus per probe. In control oocytes, homologous centromeres were efficiently paired throughout all stages of meiosis in the germarium (Figure 3A). In *GL00409/*NGTA oocytes, pairing was defective (Figure 3B). Those centromeres that were able to successfully pair, still failed to cluster (Figure 3C). These results suggest that there are defects in both centromere pairing and clustering, consistent with a defect in sister centromere cohesion. We also tested if a cohesin defect was persistent, and therefore would result in increased CID foci in metaphase I oocytes. The variability in CID foci number was greater in the experimental group, but the mean was not significantly different from the control (Figure 2H, I).

These data show that during early meiotic prophase, CENP-C is responsible for recruiting MIS12 and for centromere clustering and pairing. As these defects were observed in the presence of constant centromeric CID levels, these CENP-C functions appear to be distinct from centromere maintenance.

Prophase CENP-C plays a critical role in maintenance of centromeres and kinetochores.

To test the function of CENP-C loaded during mid-late prophase, we used the *mata* promoter to express *Cenp-C* shRNA (Figure 1, *GL00409/mata*). The *GL00409/mata* females were sterile, although this could be due to the lack of CENP-C in the early embryo. To investigate the effects on meiosis I, stage 14 *GL00409/mata* oocytes were analyzed for meiotic phenotypes. The level of CENP-C at the centromeres was reduced to approximately 20% of WT levels (Figure 4A, B). We also examined the phenotype of a hypomorphic allele, *Cenp-C*$^{Z3\text{-}4375}$ [40]. When *Cenp-C*$^{Z3\text{-}4375}$ was heterozygous to a null allele (*Cenp-C*^{IR35}), centromeric CENP-C levels in oocytes were reduced, though not to the same levels as with *GL00409* (Figure 4A, B). The intensity of CID at the centromeres, despite observing no significant changes when *GL00409* was expressed in early stages of meiosis (Figure 2), was mildly reduced by 25% in *GL00409/mata* oocytes compared to control levels (Figure 4A, C). A similar reduction in centromeric CID was observed in the *Cenp-C*$^{Z3\text{-}4375}$/*Cenp-C*^{IR35} mutant oocytes. These results suggest that CENP-C might play a role in stabilization of CID late in meiotic prophase or in metaphase I.

To determine if the loss of CENP-C affects kinetochore assembly, we quantified the intensity of MIS12 and SPC105R in mature oocytes. Consistent with the reduction in CENP-C levels, we observed approximately a 75% reduction in MIS12 levels and a 90% reduction in SPC105R in *GL00409/mata* oocytes (Figure 4D-G). Consistent with the loss of SPC105R recruitment, we observed an increase in the distance between

238 centromeres and microtubules (Figure S 5), which has previously been observed when
239 SPC105R is depleted [41]. These results suggest CENP-C recruits MIS-12, which then
240 recruits SPC105R.

241 To determine whether the loss of CENP-C in oocytes affected chromosome
242 segregation at meiosis I, we assayed for bi-orientation of homologous chromosomes
243 using FISH. We observed a dramatic increase in bi-orientation errors (primarily mono-
244 orientation) in *GL00409/mata* oocytes compared to the control (Figure 5). Bi-orientation
245 errors were also elevated in *Cenp-C*$^{Z3\text{-}4375}$ */Cenp-C*^{IR35} mutant oocytes, though not to
246 the same extent as the shRNA-expressing oocytes. These spindle attachment errors
247 could indicate that CENP-C plays a direct role in error correction, but more likely has an
248 indirect effect due to the function of CENP-C in kinetochore assembly.
249

250 **Rescue of the CENP-C phenotype by late prophase expression of a wild-type**
251 **allele**

252 The defects observed in *GL00409*/*mata* females suggest that prophase CENP-C
253 expression is required for meiosis and fertility. To determine if prophase-expressed
254 CENP-C was functional in meiosis, we tested whether expression of a transgene in late
255 prophase could complement the *Cenp-C* RNAi or mutant phenotypes. Two *UASP* –
256 regulated transgenes expressing *Cenp-C* were used for these experiments, one GFP-
257 tagged and another HA-tagged. These two constructs differ at the 5'UTR, which is
258 present in *GFP-Cenp-C* and carries the target sequence for *GL00409*. In contrast, *HA-*
259 *Cenp-C* lacks the 5'UTR and is therefore resistant to knockdown by *GL00409.*

If prophase expression of CENP-C is functional, it should be able to rescue phenotypes observed in *Cenp-C*$^{Z3\text{-}4375}$*/Cenp-C*^{IR35} females. The *HA-Cenp-C* transgene was shown to be functional by co-expressing it in *GL00409*/*mata* oocytes. This resulted in localization of HA-CENP-C to the centromeres and restoration of MIS12 and SPC105R localization in *GL00409/mata* oocytes (Figure 4D-G). In addition, the biorientation defects in *GL00409/mata* oocytes were rescued by expression of HA-CENP-C (Figure 5).

Despite the rescue of the RNAi phenotypes, expression of HA-CENP-C using *mata* caused sterility (Table 2). Using *P{w[+mC]=osk-GAL4::VP16}A11* (referred to as *oskGal4*), which has an expression pattern similar to *matα* but at lower levels [42], resulted in fertile females (Table 2). These results suggest overexpression of CENP-C leads to loss of fertility. The females expressing HA-CENP-C had normal oocytes at metaphase I, making it likely that the defect causing sterility is after meiosis I, possibly during embryonic mitosis. Using *oskGal4*, we found that expression of HA-CENP-C or GFP-CENP-C rescued the sterility of *Cenp-C*$^{Z3\text{-}4375}$*/Cenp-C*^{IR35} mutant females (Table 2). In addition, SPC105R localization was restored (Figure 4F-G) and the biorientation defects in *Cenp-C*$^{Z3\text{-}4375}$*/Cenp-C*^{IR35} mutant females was rescued (Figure 5). These results show that late prophase expression of CENP-C contributes to kinetochore function in meiosis I.

The RNAi resistance of the *HA-Cenp-C* transgene can be used to express mutant variants in the absence of wild-type CENP-C. Previous studies have shown that the C-terminal domain of *Drosophila* CENP-C interacts with the centromere components CID and CAL1 [17, 23]. To determine what domains of CENP-C are required for

prophase loading in oocytes, we generated two *Cenp-C* transgenes expressing either the N-terminal (aa 1-788, *Cenp-C*^{N}) or C-terminal (789–1411, *Cenp-C*^{C}) domain of CENP-C. The N-terminal domain was not detected by fluorescence microscopy, suggesting it is either unstable or does not localize. In contrast, CENP-C^{C} was loaded during prophase (Figure S 2), localized to the centromeres (Figure S 5), but failed to recruit SPC105R or MIS12 (Figure 4D-G). These results support the conclusion that the C-terminal domain of CENP-C is required for centromere localization, while the N-terminal domain promotes recruitment of MIS12 and the rest of the kinetochore.

Centromeric CENP-C exchanges during prophase I

Our results have shown that CENP-C loading during prophase is required for fertility. To test the relationship between the loading and unloading of CENP-C during prophase, females were generated that expressed *GL00409* and *HA-Cenp-C* under the control of *mata,* and *GFP-Cenp-C* under the control of its own promoter (Figure 6A). GFP-CENP-C was expected to be expressed at all stages of the germline but, due to containing the 5' UTR, was sensitive to the shRNA in meiotic prophase. In contrast, expression of the HA-CENP-C would begin in early prophase and resistant to the co-expressed shRNA because it lacks the 5'UTR. This setup allowed us to simultaneously compare the unloading and loading of centromeric CENP-C during prophase. In particular, is unloading of centromeric CENP-C dependent upon loading from the cytoplasmic pool of CENP-C?

In females expressing GFP-CENP-C and *GL00409* but not HA-CENP-C, the GFP intensity was reduced over time (Figure 6B). This is consistent with the results using the CENP-C antibody (Figure 4A). In females expressing GFP-CENP-C and HA-

CENP-C, the GFP and HA signals were both maintained over time (Figure 6C). In contrast, in females expressing GFP-CENP-C, *GL00409* and HA-CENP-C, the GFP signal decreased and the HA signal increased (Figure 6D). The decrease in GFP signal after induction of shRNA expression was greater when HA-CENP-C was expressed than in females not expressing HA-CENP-C. This observation suggests the actions of an exchange mechanism during prophase that is sensitive to cytoplasmic levels of CENP-C. We propose that the unloading of centromeric CENP-C depends on the availability of a replacement. Notably, while the GFP signal at the centromeres in oocytes drops dramatically at the onset of HA and shRNA expression, low but significant GFP signals were still observed in stage 14 oocytes (Figure 6D). These results suggest that, although most CENP-C is exchanged during prophase, there is a small pool of CENP-C that is stably maintained throughout meiosis. Similar results were observed with the *HA-CenpC*^{C} mutant (Figure 6E), which suggests that exchange of CENP-C is not dependent on the N-terminal domain of the protein.

DISCUSSION

Prophase dynamics of centromere proteins

In *Drosophila*, centromere maintenance involves three proteins, CID, CAL1, and CENP-C, and occurs during late M or G1 (see Introduction). We show here that only CENP-C is loaded during meiotic prophase. The prophase CENP-C population is required for at least two meiotic functions: sister centromere cohesion and kinetochore assembly. Reductions in CENP-C levels were not accompanied by similar decreases in CID at the centromeres, showing that prophase-loaded CENP-C is not required to maintain the centromeres.

We observed CENP-C unloading at a higher rate when there was a cytoplasmic source of replacement CENP-C. This indicates that an exchange reaction may be operating and without new sources of CENP-C, the dynamics are reduced. The C-terminal domain of CENP-C had the same dynamic properties during prophase as the full-length protein. This part of the protein also contains the elements required to interact with CID and CAL1 for centromere maintenance [17, 18, 25]. Some evidence in mammals, however, suggests CENP-C has both CENP-A-dependent and independent localization mechanisms, although in most of these studies, loading during G2 is not specifically addressed [43]. CENP-C loading occurs while CID is not loaded and CAL1 is unloaded. In addition, CAL1 was absent in metaphase I, in contrast to observations in mitotic cells [7, 16]. Thus, prophase loading of CENP-C may involve a mechanism that involve factors other than CAL1 and CID. For example, CDK1 has been implicated in CENP-C dynamics in chicken and human cells [44].

We did not observe incorporation of CID during prophase, which is consistent with studies on CENP-A in mouse oocytes [28]. However, it has been reported that CID is incorporated during meiotic prophase of *Drosophila* females [45]. We suspect the difference between our study and the prior study is how incorporation was measured. The prior studies used changes in fluorescence intensity, which could be affected by changes in the environment of the centromere as the oocyte develops (e.g. the oocyte gets larger, the chromatin changes). We used pulsed expression, which allows for direct observation of the incorporation of newly synthesized centromere proteins.

Early prophase function: centromere clustering and cohesion

When CENP-C was depleted from early prophase oocytes, we observed an increased number of centromere foci. CID levels were not reduced by *Cenp-C* RNAi, suggesting these phenotypes most likely result from early prophase loss of CENP-C. Our results suggest the increased CID foci phenotype could be due to a loss of centromeric cohesion because we also observed an increase in sister chromatid nondisjunction. These observations are consistent with and extend prior studies on *Cenp-C* [40]. These authors also found that *Cenp-C*$^{Z3\text{-}4375}$ mutant females have defects in centromere clustering in pachytene oocytes (region 3 of the germarium). The centromere clustering and pairing phenotypes are similar to a hypomorphic allele of replication protein *mcm5* that was associated with loss of SMC1 at the centromeres [46]. Thus, we propose that CENP-C is required to recruit or maintain cohesion. A recruitment function of CENP-C could occur when cohesion is established in S-phase [38]. Alternatively, our results show striking similarities to the known roles of mammalian

and yeast CENP-C in recruiting Moa1 or Meikin [47, 48], which are protectors of centromeric cohesion and particularly important for meiosis I.

Late prophase function: kinetochore assembly

Depletion of prophase CENP-C resulted in phenotypes associated with loss of the kinetochore. This includes loss of MIS12 and SPC105R when CENP-C was depleted in prophase. These results show that CENP-C is required for most or all kinetochore assembly, consistent with studies in *Drosophila* mitotic cells [19, 24, 25]. The C-terminal domain of CENP-C was recruited to the centromere but failed to assemble a kinetochore. Thus, the N-terminal domain of CENP-C appears to interact with MIS12 and recruit the rest of the kinetochore, consistent with previous studies in *Drosophila* [23, 27]. These results also show that unlike CID/CENP-A, CENP-C that is sufficient for centromere maintenance is not sufficient for kinetochore assembly. Studies in vertebrate cells have shown that CENP-C is dynamic during interphase but stable in metaphase [31, 49]. If the same is true here, then prophase loaded CENP-C provides a platform for kinetochore assembly at the beginning of meiotic prometaphase in oocytes.

Implications of CENP-C prophase loading

CENP-A /CID is remarkably stable [50, 51]. Therefore, even though our results show that CID/CENP-A is not loaded during extended prophase in oocytes, it appears to be adapted for this by being extremely stable. CENP-C must be loaded during prophase, making it among a small number of proteins that are required for kinetochore function but are loaded prior to metaphase I. Why CENP-C but not CID/CENP-A must be loaded during prophase is not known. It is possible that more CENP-C is needed for kinetochore assembly than centromere maintenance. Loading CENP-C during

prophase could be a mechanism to establish a stable and invariant platform to regulate assembly of a specific size of kinetochore in prometaphase. The requirement for CENP-C prophase loading could affect the health of aging oocytes. If loading of CENP-C is compromised in older oocytes that have spent more time in prophase, our results show that both sister chromatid cohesion and kinetochore assembly could be affected.

Acknowledgements

We thank Marina Druzhinina for technical assistance, Christian Lehner for providing Drosophila stocks and antibodies. We also thank Sarah Radford for early work on this project. We thank the Bloomington *Drosophila* Stock Center (NIH P40OD018537) and the TRiP project at Harvard Medical School for providing fly stocks used in this study. J.F was supported by a NIH IRACDA post-doctoral Fellowship. This work was supported by NIH grant GM101955 to K.S.M.

METHODS

Drosophila strains and genetics

Drosophila crosses and stocks were kept at 25°C on standard medium. Fly stocks were obtained from the Bloomington Stock Center or the Transgenic RNAi Project at Harvard Medical School [TRiP, Boston, MA, USA, flyrnai.org], and information about the genetic loci can be found on FlyBase [flybase.org]. *Drosophila* lines expressing a short hairpin RNA (shRNA) were obtained from the Bloomington Stock Center. Expression of the shRNA was controlled by the Upstream Activating Sequence (UAS), which is activated by expression of GAL4 under the control of a tissue-specific enhancer [1]. Five *Gal4* strains were used in this study, four of which were germline-specific: *P{matalpha4-GAL-VP16}V37* and *P{w[+mC]=osk-GAL4::VP16}A11* promote expression after zygotene, *P{GAL4-nos.NGT}A* promotes expression only in the germarium (during prophase I), and *P{GAL4: :VP16-nos.UTR}CG6325*^{MVD1} promotes expression throughout the whole germline. In addition, heat shock was used to induce expression of transgenes using *P{GAL4-Hsp70,PB}89-2-1.*

The shRNA used to reduce *Cenp-C* expression, *GL00409*, is located on chromosome II. To measure the extent of the *Cenp-C mRNA* knockdown, total RNA was extracted from stage 14 oocytes expressing *GL00409* with *P{matalpha4-GAL-VP16}V37* using the TRIzol Reagent (Life Technologies). cDNA was made using the High-Capacity cDNA Reverse Transcription kit (Applied Biosystems). TaqMan Gene Expression Assays (Life Technologies) were used to measure expression levels of CENP-C. RT-qPCR was done on a StepOnePlus (Life Technologies) real-time PCR system and results showed that the *Cenp-C* RNAi expressed only 4% of wild-type RNA.

In addition, CAL1 was knocked down using shRNA *GL01832* and CDK1 was knocked down using shRNA *HMS01531*, both located on chromosome II.

Cencp-C$^{Z3\text{-}4375}$ is a homozygous-viable allele that has a missense mutation in the CENP-C motif, changing a proline amino acid to a serine at position 1116. [40]. For the analysis of *Cenp-C*$^{Z3\text{-}4375}$, trans heterozygous mutant strains were used, with one chromosome carrying either the *Cenp-C*^{IR35} or *Cenp-C*^{pr141} mutations. The *Cenp-C*^{IR35} mutation is a premature stop codon at position 858 before the CENP-C motif and Cupin domain, resulting in a deletion of these regions [52]. The *Cenp-C*^{pr141} mutation is a premature stop codon at position 1107 within the CENP-C motif [52], resulting in a partial deletion of the CENP-C motif and the rest of the protein.

HA- and GFP-tagged transgenes

The coding region of cDNA clone FI18815 was PCR amplified and cloned in frame into pENTR4 (HiFi assembly, NEB) and then into pPHW using Clonase (Life Tech.). The target sequence for *GL00409* is located in the 5'UTR of *Cenp-C* and, therefore, this transgene is RNAi resistant. The GFP-CENP-C is similar but contains the 5'UTR sequences upstream of the GFP sequence, and thus is RNAi sensitive. MIS12 localization was observed using a UASP regulated GFP-fusion transgene [53].

Fertility trials, nondisjunction, and crossover assays

The *GL00409 Cenp-C* shRNA was tested for fertility and chromosome segregation errors by crossing females expressing the shRNA to *yw/ B*^{S} *Y* males. The aneuploid genotypes that survive are *y/y/ B*^{S} *Y* (Bar-eyed females) and *y w / 0* (wild-type males). Because half the aneuploid progeny have lethal genotypes, aneuploidy was

calculated by multiplying the number of aneuploid progeny by two and dividing by the total number of progeny.

Sister chromatid aneuploidy was tested by crossing *y w/ Bwinscy* females expressing the shRNA to *v f B ^ Y* males. If aneuploidy occurs among homologous chromosomes, the expected genotypes that survive are *y w/Bwinscy* and *O/ v f B ^ Y*. Aneuploidy among sister chromatids is detected by the genotypes *y w/y w* (non-bar-eyed females) or *Bwinscy/Bwinscy* (Bar-eyed females). Because the O/ *v f B ^ Y* genotype arises from both MI or MII nondisjunction, only the *y w/y w* and *Bwinscy/Bwinscy* progeny were used to determine the sister chromatid aneuploidy frequency. Therefore, the number of aneuploid progeny counted was multiplied by four and divided by the total number of progeny in order to measure sister chromatid aneuploidy.

In order to observe the role of CENP-C in crossing over, females were generated that expressed the shRNA and were heterozygous for four genetic markers on chromosome III: *st, cu, e* and *ca*. These females were crossed to a strain carrying all the recessive traits and the frequency of the recombinants was scored.

Cytology and immunofluorescence of early prophase oocytes

For immunolocalization experiments in the germaria, mated females were aged for 1-2 days at 25°C. In one well of a two well plate, 10-15 ovaries were dissected using 1x Robb's media and then were transferred to the second well containing fresh media. A tungsten needle was used to break open the ovary sheath and tease the ovarioles apart. The dissected ovaries were transferred to a 1.5 mL Eppendorf tube with 4% formaldehyde in 500ul of Buffer A as described [54]. The ovaries were nutated at room

473 temperature for 10 minutes, then were washed four times before adding the primary
474 antibodies. The next day, following four washes, secondary antibodies were added and
475 incubated at room temperature for 4 hours.

476 **Cytology and immunofluorescence of metaphase I oocytes**

477 For immunolocalization experiments in pro-metaphase I oocytes (stages 13-14),
478 we used the immunocytochemical protocol as described [55]. I brief, 100-200 females
479 were aged 2-3 days with males in yeasted vials [56]. Oocytes were collected by pulsing
480 the females in a blender and then separating the oocytes from the bulk fly tissues using
481 a mesh. Oocytes were fixed in 5% formaldehyde solution for 2.5 minutes, and then
482 equal amounts of heptane were added and the oocytes were vortexed for 30 seconds.
483 The membranes were removed by rolling the oocytes between a coverslip and the
484 frosted part of a glass slide. These oocytes were incubated in PBS/1% Triton X-100 for
485 two hours, then washed in PBS/0.05% Triton X-100. The oocytes were blocked in
486 PBS/0.1% Tween 20/0.5% BSA (PTB) for one hour, and then incubated with primary
487 antibodies overnight. Oocytes were washed the next day in PTB and incubated with
488 secondary antibodies for 4 hours at room temperature.

489 Tissues were mounted for confocal imaging using SlowFade Gold (Invitrogen). A
490 Leica TPS SP8 confocal microscope with a 63X, N.A. 1.4 lens was used to visualize
491 fluorescent tags using different colored lasers. Images were imaged by collecting
492 sections throughout the germarium or stage 14 oocyte spindle, using parameters
493 optimized by the Leica Confocal software based on the lens and wavelength. Images
494 were analyzed as image stacks and presented as maximum projections whole
495 germarium, cells or spindles.

Antibodies

An antibody against CENP-C made in guinea pig was made by generating a clone expressing amino acids 502-939 (Genscript). This guinea pig anti-CENP-C was used at 1:1000. Additional primary antibodies were rat anti-CID (Active motif, 1:100), rabbit anti-CID (Active motif, 1:100), rabbit anti-SPC105R (1:4000) [57], rabbit anti-GFP (Invitrogen, 1:400), rat anti-HA (Roche, 1:50), mouse anti-C(3)G (1:500) [58], two mouse anti-ORB antibodies, 6H4 and 4H8 (1:100 for each) [59] and mouse anti-α tubulin DM1A conjugated directly to FITC (Sigma, 1:50). The secondary antibodies that were used were Cy3, Alexa 546, Alexa 633, or Alexa 647 from Jackson Immunoresearch Laboratories, and Alexa 488 from Invitrogen. The oocytes were stained with Hoechst 33342 at 1:10,000 (10 μg/ml). FISH probes were obtained from IDT where the X359 repeat was labeled with Alexa 594, the dodeca repeat was labeled with Cy5, and the AACAC repeat was labeled with Cy3.

Quantification and statistical analysis

Aneuploidy in flies expressing the *Cenp-C* shRNA with NGTA was compared to that of the control group and a t-test was done to determine if the difference is statistically significant (p-value < 0.05). Sister chromatid aneuploidy in flies expressing the *Cenp-C* shRNA with NGTA was compared to that of the control group and a t-test was used to determine whether the difference was statistically significant (p-value < 0.05). The percent of crossovers at each position was compared to that of the control group using a t-test, and if the difference was statistically significant (p-value < 0.05),

518 then this indicated that elevated or reduced recombination occurred at that specific
519 location.

520 Quantification of CID foci and protein localization in both the germarium and in
521 stage 14 oocytes was measured using the Imaris Software. To quantify centromere foci,
522 the automated spots detection feature of Imaris was used. A spot with a XY diameter of
523 0.20 μm, a Z diameter of 1.00 μm, and a physical interaction with the DNA was counted
524 as a centromere. A t-test was done to compare the number of centromere foci in flies
525 expressing the knockdown to the number in the control group using a p-value < 0.05 to
526 indicate statistical significance.

527 To measure the localization of proteins to the centromere or the nucleus in *Cenp-*
528 *C* RNAi, intensity experiments were performed using Imaris. The Imaris software was
529 utilized to measure protein intensity at the centromere of the oocyte, using CID as the
530 centromere marker. Spots were chosen in random somatic cells to quantify the intensity
531 of the background. The intensity of the protein at the centromere was divided by the
532 background and a t-test was used to determine whether the centromere protein intensity
533 was reduced with a loss of CENP-C.

534 Intensity experiments were also performed to measure localization of MIS12,
535 SPC105R, or CENP-C to the centromere at stage 14 using a similar protocol. However,
536 background intensity was measured in the oocyte cytoplasm as opposed to measuring
537 the background in the somatic cells for germarium images. A t-test was used to
538 determine whether the intensity of the protein of interest at the centromere normalized
539 to the background was reduced with a loss of CENP-C using a p-value <0.05 to indicate
540 statistical significance.

541

542

Table 1: Fertility, nondisjunction and crossing over in *Cenp-C* RNAi females

	Fertility	Nondisjunction (NDJ)		Recombination (% of control)			
	Offspring per female (# of females)	Homologous Chromosome NDJ (# of offspring)	Sister Chromatid NDJ (# of offspring)	*st-cu (m.u.)*	*cu-e (m.u.)*	*e-ca (m.u.)*	# of progeny
Control	24.3 (105)	0.25% (1590)	0.5% (2696)	4.4 (100%)	2.2 (100 %)	29.4 (100 %)	2853
GL00409 / NGTA	10.0 (240)	7.0% (1658)	2.6% (1164)	9.4 (226%)	21.1 (101 %)	22.9 (81%)	1668
HMJ21500/ NGTA	3.3 (133)	7.6 (1213)	ND	ND	ND	ND	ND
GL00409 / MVD1	0.27 (105)	0% (54)	- [a]	-	-	-	-

[a] not enough progeny to accurately measure nondisjunction or crossing over

549

550 **Table 2: Fertility in *Cenp-C* RNAi, mutant and transgenic females**

551

Genotype	Offspring per female (# of females)
Control (*w-*)	22.93 (90)
HA-Cenp-C ; mata	0.58 (325)
HA-Cenp-C ; oskar	23.15 (125)
EGFP-Cenp-C ; mata	0.14 (150)
EGFP-Cenp-C ; oskar	18.11 (65)
$Cenp\text{-}C^{Z}/+$	11.5 (120)
$Cenp\text{-}C^{IR35}/+$	13.58 (160)
$Cenp\text{-}C^{pr141}/+$	19.82 (105)
$Cenp\text{-}C^{Z}/Cenp\text{-}C^{Z}$	1.46 (120)
$Cenp\text{-}C^{Z}/ Cenp\text{-}C^{IR35}$	0.06 (270)
$Cenp\text{-}C^{Z}/ Cenp\text{-}C^{pr141}$	0.25 (70)
$Cenp\text{-}C^{Z}/ Cenp\text{-}C^{IR35}$; *HA-Cenp-C; mat a*	1.358 (460)
$Cenp\text{-}C^{Z}/ Cenp\text{-}C^{IR35}$; *HA-Cenp-C ; oskar*	15.22 (180)
$Cenp\text{-}C^{Z}/ Cenp\text{-}C^{pr141}$; *EGFP-Cenp-C; mata*	0.21 (125)
$Cenp\text{-}C^{Z}/ Cenp\text{-}C^{pr141}$; *EGFP-Cenp-C ; oskar*	11.27 (130)
GL00409 ; mata	0 (120)
GL00409 ; oskar	10.81 (90)
GL00409; HA-Cenp-C; mat a	0.08 (430)
GL00409; HA-Cenp-C; oskar	26.72 (65)

552

553

Supplementary Figures

Figure S 1: Expression pattern of NGTA. Related to Figure 1 and 2

The expression pattern of **(A)** *P{GAL4-nos.NGT}* and **(B)** *P{GAL4::VP16-nos.UTR}CG6325MVD1* using *UASP-β-galactosidase* as a reporter. Arrowheads indicate anterior tip of the ovariole, where the germarium is located, and the blue stain indicates where each GAL4 promotes expression.

Figure S 2: Loading of centromere proteins during oocyte meiotic prophase. Related to Figure 1 and 2

In all images, HA-CENP-C is green, the centromeres are marked with CID (red), and DNA is in blue. The scale bars represent 5 mm. **A)** Whole germarium with HA-tagged CENP-C expressed using *NGTA* or *mata*. Enriched in the oocyte is the ORB protein in white. **B)** HA-tagged CENP-C or CENP-C^C was expressed using *mata*. **C)** HA-CENP-C was expressed using *hsp70-Gal4*. Oocytes were collected and fixed 6 hours after a 1-hour incubation at 37°C.

Figure S 3: CAL1 localization in stage 14 oocytes. Related to 1 and 4

EGFP-tagged CENP-C or CAL1 (grey in single channel, green in merge) in stage 14 oocytes. The DNA is blue, microtubules in red, and the scale bars represent 5 mm. **A)** Localization of GFP-tagged CENP-C expressed using the *MVD1* promoter. The centromeres were detected using CID (white). **B)** Localization of GFP-tagged CAL1

using the *MVD1* promoter. The centromeres were detected using an antibody against CENP-C (white). **C)** Localization of GFP-tagged CAL1 using the endogenous *cal1* promoter. The centromeres were detected using an antibody against CENP-C (white).

Figure S 4: SC assembly in when CENP-C is depleted in prophase. Related to Figure 2

Confocal images of the germarium with *Cenp-C* RNAi (HMS01171) with (A) no *GAL4* and (A) *NGTA*. DNA is shown in blue, CENP-C is in red, and C(3)G is in green. The scale bar is 10 μm. CENP-C and C(3)G are shown in white in the single channel images. Region 1 of the germarium has been boxed to show increased centromeric C(3)G. The insets show single nuclei from region 1 in the germarium to show co-localization of CENP-C and C(3)G (Scale bar= 3 μm).

Figure S 5: Additional images of CENP-C localization in RNAi and transgenic oocytes. Related to Figure 4.

A) *Cenp-C* RNAi or *Cenp-C*^{Z} oocytes with CENP-C (green) and CID (red). **B)** *Cenp-C* RNAi or *Cenp-C*^{Z} oocytes expressing a *Cenp-C* transgene, with HA in red and SPC105R in green, DNA in blue, microtubules in white, and the scale bars represent 5 mm. **C)** Oocytes shown in panels A and B were assessed for KT-MT attachments. This was done by measuring the distance between each centromere and the nearest microtubule.

Literature cited

1. Nechemia-Arbely, Y., Fachinetti, D., and Cleveland, D.W. (2012). Replicating centromeric chromatin: spatial and temporal control of CENP-A assembly. Exp Cell Res *318*, 1353-1360.
2. Swartz, S.Z., McKay, L.S., Su, K.C., Bury, L., Padeganeh, A., Maddox, P.S., Knouse, K.A., and Cheeseman, I.M. (2019). Quiescent Cells Actively Replenish CENP-A Nucleosomes to Maintain Centromere Identity and Proliferative Potential. Dev Cell *51*, 35-48.e37.
3. Kixmoeller, K., Allu, P.K., and Black, B.E. (2020). The centromere comes into focus: from CENP-A nucleosomes to kinetochore connections with the spindle. Open Biol *10*, 200051.
4. Rosin, L.F., and Mellone, B.G. (2017). Centromeres Drive a Hard Bargain. Trends Genet *33*, 101-117.
5. Sridhar, S., and Fukagawa, T. (2022). Kinetochore Architecture Employs Diverse Linker Strategies Across Evolution. Front Cell Dev Biol *10*, 862637.
6. Jansen, L.E., Black, B.E., Foltz, D.R., and Cleveland, D.W. (2007). Propagation of centromeric chromatin requires exit from mitosis. J Cell Biol *176*, 795-805.
7. Mellone, B.G., Grive, K.J., Shteyn, V., Bowers, S.R., Oderberg, I., and Karpen, G.H. (2011). Assembly of Drosophila centromeric chromatin proteins during mitosis. PLoS Genet *7*, e1002068.
8. Schuh, M., Lehner, C.F., and Heidmann, S. (2007). Incorporation of Drosophila CID/CENP-A and CENP-C into centromeres during early embryonic anaphase. Curr Biol *17*, 237-243.
9. Camahort, R., Li, B., Florens, L., Swanson, S.K., Washburn, M.P., and Gerton, J.L. (2007). Scm3 is essential to recruit the histone h3 variant cse4 to centromeres and to maintain a functional kinetochore. Molecular cell *26*, 853-865.
10. Chen, C.C., Dechassa, M.L., Bettini, E., Ledoux, M.B., Belisario, C., Heun, P., Luger, K., and Mellone, B.G. (2014). CAL1 is the Drosophila CENP-A assembly factor. J Cell Biol *204*, 313-329.
11. Foltz, D.R., Jansen, L.E., Bailey, A.O., Yates, J.R., 3rd, Bassett, E.A., Wood, S., Black, B.E., and Cleveland, D.W. (2009). Centromere-specific assembly of CENP-a nucleosomes is mediated by HJURP. Cell *137*, 472-484.
12. Williams, J.S., Hayashi, T., Yanagida, M., and Russell, P. (2009). Fission yeast Scm3 mediates stable assembly of Cnp1/CENP-A into centromeric chromatin. Mol Cell *33*, 287-298.
13. Sanchez-Pulido, L., Pidoux, A.L., Ponting, C.P., and Allshire, R.C. (2009). Common ancestry of the CENP-A chaperones Scm3 and HJURP. Cell *137*, 1173-1174.
14. Dunleavy, E.M., Roche, D., Tagami, H., Lacoste, N., Ray-Gallet, D., Nakamura, Y., Daigo, Y., Nakatani, Y., and Almouzni-Pettinotti, G. (2009). HJURP is a cell-cycle-dependent maintenance and deposition factor of CENP-A at centromeres. Cell *137*, 485-497.
15. Pidoux, A.L., Choi, E.S., Abbott, J.K., Liu, X., Kagansky, A., Castillo, A.G., Hamilton, G.L., Richardson, W., Rappsilber, J., He, X., et al. (2009). Fission yeast Scm3: A CENP-A receptor required for integrity of subkinetochore chromatin. Molecular cell *33*, 299-311.
16. Erhardt, S., Mellone, B.G., Betts, C.M., Zhang, W., Karpen, G.H., and Straight, A.F. (2008). Genome-wide analysis reveals a cell cycle-dependent mechanism controlling centromere propagation. J Cell Biol *183*, 805-818.
17. Medina-Pritchard, B., Lazou, V., Zou, J., Byron, O., Abad, M.A., Rappsilber, J., Heun, P., and Jeyaprakash, A.A. (2020). Structural basis for centromere maintenance by Drosophila CENP-A chaperone CAL1. EMBO J *39*, e103234.
18. Schittenhelm, R.B., Althoff, F., Heidmann, S., and Lehner, C.F. (2010). Detrimental incorporation of excess Cenp-A/Cid and Cenp-C into Drosophila centromeres is prevented by limiting amounts of the bridging factor Cal1. J Cell Sci *123*, 3768-3779.

19. Orr, B., and Sunkel, C.E. (2011). Drosophila CENP-C is essential for centromere identity. Chromosoma *120*, 83-96.
20. Screpanti, E., De Antoni, A., Alushin, G.M., Petrovic, A., Melis, T., Nogales, E., and Musacchio, A. (2011). Direct binding of Cenp-C to the Mis12 complex joins the inner and outer kinetochore. Curr Biol *21*, 391-398.
21. Petrovic, A., Keller, J., Liu, Y., Overlack, K., John, J., Dimitrova, Y.N., Jenni, S., van Gerwen, S., Stege, P., Wohlgemuth, S., et al. (2016). Structure of the MIS12 Complex and Molecular Basis of Its Interaction with CENP-C at Human Kinetochores. Cell *167*, 1028-1040 e1015.
22. Tanaka, K., Chang, H.L., Kagami, A., and Watanabe, Y. (2009). CENP-C functions as a scaffold for effectors with essential kinetochore functions in mitosis and meiosis. Dev Cell *17*, 334-343.
23. Liu, Y., Petrovic, A., Rombaut, P., Mosalaganti, S., Keller, J., Raunser, S., Herzog, F., and Musacchio, A. (2016). Insights from the reconstitution of the divergent outer kinetochore of Drosophila melanogaster. Open Biol *6*, 150236.
24. Przewloka, M.R., Zhang, W., Costa, P., Archambault, V., D'Avino, P.P., Lilley, K.S., Laue, E.D., McAinsh, A.D., and Glover, D.M. (2007). Molecular analysis of core kinetochore composition and assembly in Drosophila melanogaster. PloS one *2*, e478.
25. Przewloka, M.R., Venkei, Z., Bolanos-Garcia, V.M., Debski, J., Dadlez, M., and Glover, D.M. (2011). CENP-C is a structural platform for kinetochore assembly. Curr Biol *21*, 399-405.
26. Venkei, Z., Przewloka, M.R., and Glover, D.M. (2011). Drosophila Mis12 complex acts as a single functional unit essential for anaphase chromosome movement and a robust spindle assembly checkpoint. Genetics *187*, 131-140.
27. Richter, M.M., Poznanski, J., Zdziarska, A., Czarnocki-Cieciura, M., Lipinszki, Z., Dadlez, M., Glover, D.M., and Przewloka, M.R. (2016). Network of protein interactions within the Drosophila inner kinetochore. Open Biol *6*, 150238.
28. Smoak, E.M., Stein, P., Schultz, R.M., Lampson, M.A., and Black, B.E. (2016). Long-Term Retention of CENP-A Nucleosomes in Mammalian Oocytes Underpins Transgenerational Inheritance of Centromere Identity. Curr Biol *26*, 1110-1116.
29. Mihajlovic, A.I., and FitzHarris, G. (2018). Segregating Chromosomes in the Mammalian Oocyte. Curr Biol *28*, R895-R907.
30. Toth, A., and Jessberger, R. (2016). Oogenesis: Ageing Oocyte Chromosomes Rely on Amazing Protein Stability. Curr Biol *26*, R329-331.
31. Hemmerich, P., Weidtkamp-Peters, S., Hoischen, C., Schmiedeberg, L., Erliandri, I., and Diekmann, S. (2008). Dynamics of inner kinetochore assembly and maintenance in living cells. J Cell Biol *180*, 1101-1114.
32. Das, A., Black, B.E., and Lampson, M.A. (2020). Maternal inheritance of centromeres through the germline. Curr Top Dev Biol *140*, 35-54.
33. Rorth, P. (1998). Gal4 in the Drosophila female germline. Mech Dev *78*, 113-118.
34. Radford, S.J., Jang, J.K., and McKim, K.S. (2012). The Chromosomal Passenger Complex is required for Meiotic Acentrosomal Spindle Assembly and Chromosome Bi-orientation. Genetics *192*, 417-429.
35. Sugimura, I., and Lilly, M.A. (2006). Bruno inhibits the expression of mitotic cyclins during the prophase I meiotic arrest of Drosophila oocytes. Dev Cell *10*, 127-135.
36. Baker, B.S., and Hall, J.C. (1976). Meiotic mutants: genetic control of meiotic recombination and chromosome segregation. In The Genetics and Biology of Drosophila, Volume 1a, M. Ashburner and E. Novitski, eds. (New York: Academic Press), pp. 351-434.
37. Hughes, S.E., Hemenway, E., Guo, F., Yi, K., Yu, Z., and Hawley, R.S. (2019). The E3 ubiquitin ligase Sina regulates the assembly and disassembly of the synaptonemal complex in Drosophila females. PLoS Genet *15*, e1008161.

38. Gyuricza, M.R., Manheimer, K.B., Apte, V., Krishnan, B., Joyce, E.F., McKee, B.D., and McKim, K.S. (2016). Dynamic and Stable Cohesins Regulate Synaptonemal Complex Assembly and Chromosome Segregation. Curr Biol *26*, 1688-1698.
39. Tanneti, N.S., Landy, K., Joyce, E.F., and McKim, K.S. (2011). A Pathway for Synapsis Initiation during Zygotene in Drosophila Oocytes. Curr Biol *21*, 1852-1857.
40. Unhavaithaya, Y., and Orr-Weaver, T.L. (2013). Centromere proteins CENP-C and CAL1 functionally interact in meiosis for centromere clustering, pairing, and chromosome segregation. Proc Natl Acad Sci U S A *110*, 19878-19883.
41. Radford, S.J., Hoang, T.L., Głuszek, A.A., Ohkura, H., and McKim, K.S. (2015). Lateral and End-On Kinetochore Attachments Are Coordinated to Achieve Bi-orientation in Drosophila Oocytes. PLoS Genet *11*, e1005605.
42. Telley, I.A., Gaspar, I., Ephrussi, A., and Surrey, T. (2012). Aster migration determines the length scale of nuclear separation in the Drosophila syncytial embryo. J Cell Biol *197*, 887-895.
43. Nagpal, H., Hori, T., Furukawa, A., Sugase, K., Osakabe, A., Kurumizaka, H., and Fukagawa, T. (2015). Dynamic changes in CCAN organization through CENP-C during cell-cycle progression. Mol Biol Cell *26*, 3768-3776.
44. Watanabe, R., Hara, M., Okumura, E.I., Herve, S., Fachinetti, D., Ariyoshi, M., and Fukagawa, T. (2019). CDK1-mediated CENP-C phosphorylation modulates CENP-A binding and mitotic kinetochore localization. J Cell Biol *218*, 4042-4062.
45. Dunleavy, E.M., Beier, N.L., Gorgescu, W., Tang, J., Costes, S.V., and Karpen, G.H. (2012). The cell cycle timing of centromeric chromatin assembly in Drosophila meiosis is distinct from mitosis yet requires CAL1 and CENP-C. PLoS Biol *10*, e1001460.
46. Hatkevich, T., Boudreau, V., Rubin, T., Maddox, P.S., Huynh, J.R., and Sekelsky, J. (2019). Centromeric SMC1 promotes centromere clustering and stabilizes meiotic homolog pairing. PLoS Genet *15*, e1008412.
47. Watanabe, Y. (2012). Geometry and force behind kinetochore orientation: lessons from meiosis. Nat Rev Mol Cell Biol *13*, 370-382.
48. Nasmyth, K. (2015). A meiotic mystery: How sister kinetochores avoid being pulled in opposite directions during the first division. Bioessays *37*, 657-665.
49. Watanabe, R., Hirano, Y., Hara, M., Hiraoka, Y., and Fukagawa, T. (2022). Mobility of kinetochore proteins measured by FRAP analysis in living cells. Chromosome Res *30*, 43-57.
50. Bodor, D.L., Valente, L.P., Mata, J.F., Black, B.E., and Jansen, L.E. (2013). Assembly in G1 phase and long-term stability are unique intrinsic features of CENP-A nucleosomes. Mol Biol Cell *24*, 923-932.
51. Das, A., Iwata-Otsubo, A., Destouni, A., Dawicki-McKenna, J.M., Boese, K.G., Black, B.E., and Lampson, M.A. (2022). Epigenetic, genetic and maternal effects enable stable centromere inheritance. Nat Cell Biol *24*, 748-756.
52. Heeger, S., Leismann, O., Schittenhelm, R., Schraidt, O., Heidmann, S., and Lehner, C.F. (2005). Genetic interactions of separase regulatory subunits reveal the diverged Drosophila Cenp-C homolog. Genes Dev *19*, 2041-2053.
53. Głuszek, A.A., Cullen, C.F., Li, W., Battaglia, R.A., Radford, S.J., Costa, M.F., McKim, K.S., Goshima, G., and Ohkura, H. (2015). The microtubule catastrophe promoter Sentin delays stable kinetochore-microtubule attachment in oocytes. J Cell Biol *211*, 1113-1120.
54. McKim, K.S., Joyce, E.F., and Jang, J.K. (2009). Cytological analysis of meiosis in fixed Drosophila ovaries. Methods in molecular biology (Clifton, N.J *558*, 197-216.
55. Radford, S.J., and McKim, K.S. (2016). Techniques for Imaging Prometaphase and Metaphase of Meiosis I in Fixed Drosophila Oocytes. Journal of visualized experiments : JoVE *116*, e54666.

741 56. Gilliland, W.D., Hughes, S.F., Vietti, D.R., and Hawley, R.S. (2009). Congression of achiasmate
742 chromosomes to the metaphase plate in Drosophila melanogaster oocytes. Dev Biol *325*, 122-
743 128.
744 57. Schittenhelm, R.B., Chaleckis, R., and Lehner, C.F. (2009). Intrakinetochore localization and
745 essential functional domains of Drosophila Spc105. EMBO J *28*, 2374-2386.
746 58. Page, S.L., and Hawley, R.S. (2001). c(3)G encodes a Drosophila synaptonemal complex protein.
747 Genes & development *15*, 3130-3143.
748 59. Lantz, V., Chang, J.S., Horabin, J.I., Bopp, D., and Schedl, P. (1994). The Drosophila ORB RNA-
749 binding protein is required for the formation of the egg chamber and establishment of polarity.
750 Genes & Dev. *8*, 598-613.
751 60. Spradling, A.C. (1993). Developmental genetics of oogenesis. In The Development of Drosophila
752 melanogaster, M. Bate and A.M. Arias, eds. (Cold Spring Harbor, NY: Cold Spring Harbor
753 Laboratory Press), pp. 1-70.
754 61. Jia, D., Xu, Q., Xie, Q., Mio, W., and Deng, W.M. (2016). Automatic stage identification of
755 Drosophila egg chamber based on DAPI images. Sci Rep *6*, 18850.
756

757

758 **Figure 1**

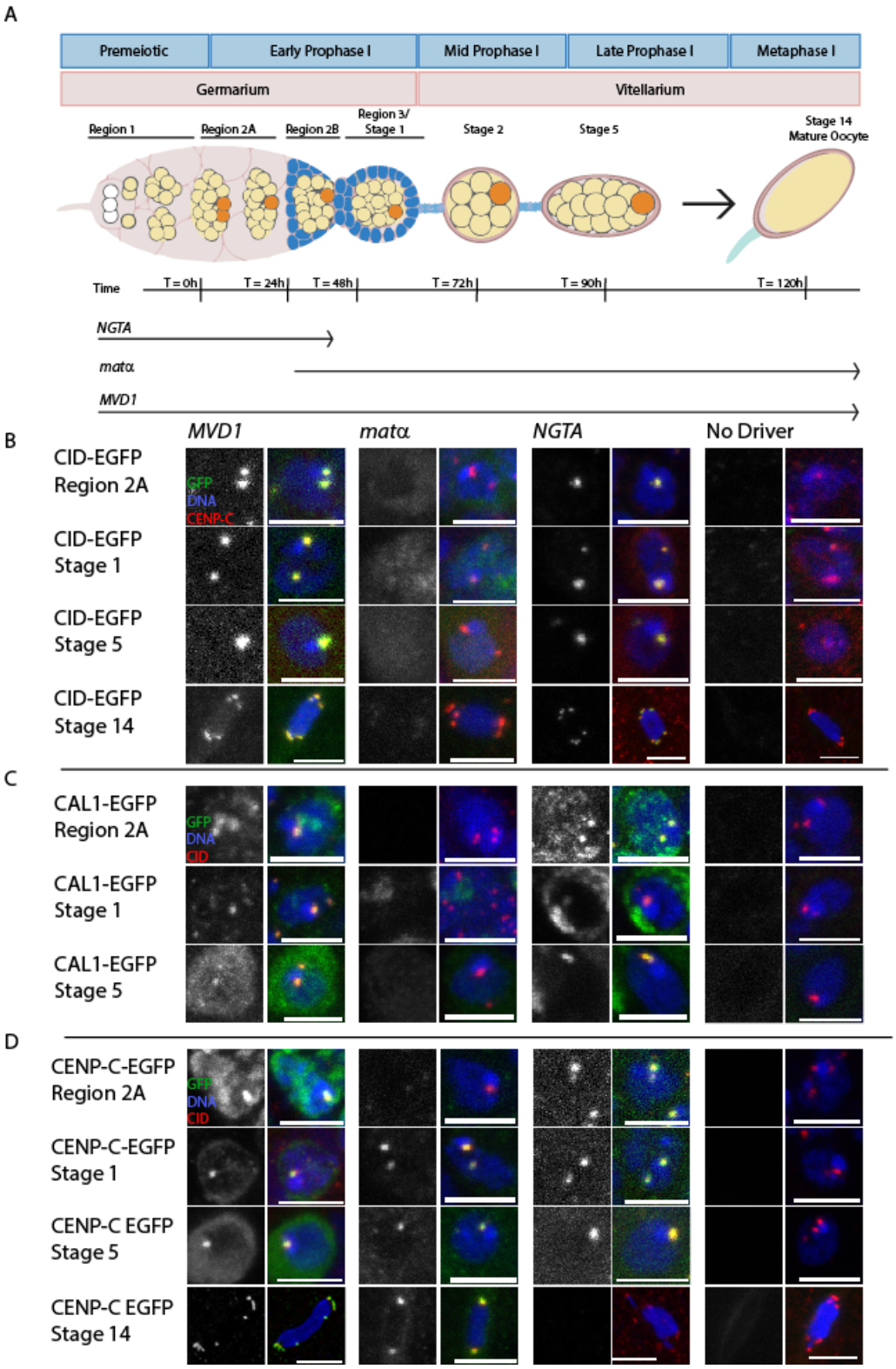

759

760

761

762 **Figure 1**

763 **Loading of centromere proteins during meiotic prophase in oocytes. A)** Oocytes
764 are generated and enter meiotic prophase in the germarium. Region 1 contains the
765 stem cell niche as well as the pre-meiotic cyst cells undergoing mitosis. Prophase I of
766 meiosis begins in region 2A. Time points are relative to the onset of meiosis [60, 61].
767 Region 3 is also known as vitellarium stage 1, and at this stage, a single oocyte
768 (orange) has been determined. *NGTA* begins expressing in the mitotic germline (region
769 1) and ends in region 3 or early in the vitellarium. *MVD1* expression begins earlier than
770 *NGTA,* being expressed in all the mitotic and meiotic stages of the germline, including
771 the stem cells. *Mata* begins expressing in region 2B or 3 and continues until stage 14,
772 the metaphase I-arrested oocyte [34]. **B)** Localization of GFP-tagged CID (green) and
773 centromeres detected using a CENP-C antibody (red). **C)** Localization of GFP-tagged
774 CAL1 (green) with the centromeres detected using a CID antibody (red). **(D)**
775 Localization of GFP-tagged CENP-C, with the centromeres detected using a CID
776 antibody (red). In all images, the DNA is blue and the scale bars are 5 mm.
777

778

Figure 2

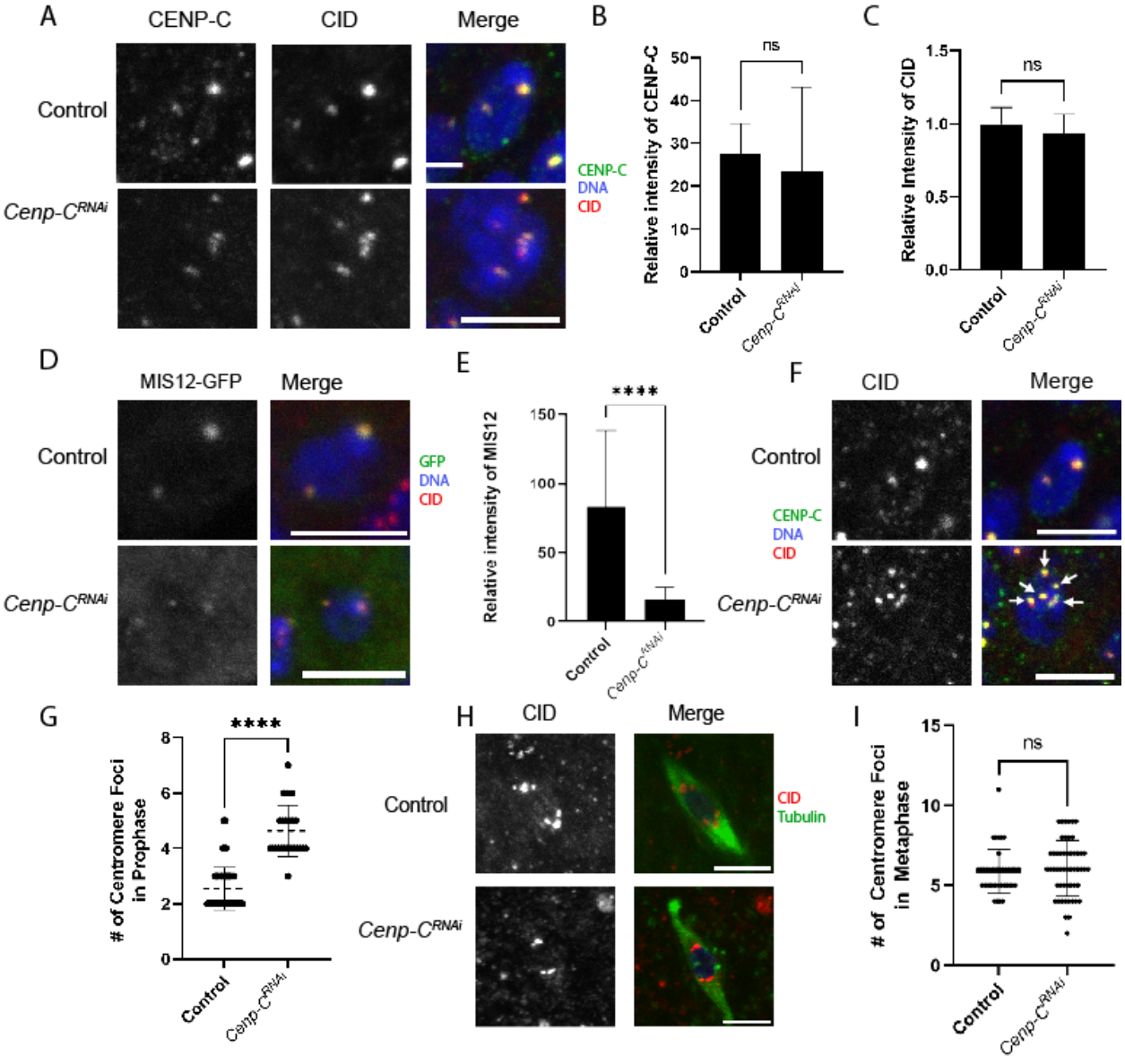

781 **Figure 2**

782 **Prophase I defects when CENP-C is depleted.** Immunocytology was performed on
783 *GL00409/NGTA* oocytes with CID (red), DNA (blue), and scale bars represent 5 mm. **A)**
784 Region 2 oocytes showing CENP-C in green. **B-C)** The intensities of CENP-C and CID
785 in region 2 were measured in *Cenp-C* RNAi and control oocytes (For B, n = 17 and 23;
786 for C, n = 11 and 29). **D)** Region 2 oocytes with MIS12-GFP in green. **E)** MIS12 intensity
787 was measured in region 2 (n = 9 and 30). **F)** CID foci in *Cenp-C* RNAi region 3 oocytes,
788 with CENP-C in green. **G)** Number of centromere foci was measured based on CID foci
789 in contact with the DNA (n = 84 and 27). **H)** tubulin (green) and CID foci (red) in *Cenp-C*
790 RNAi metaphase I oocytes. **I)** There was no increase in CID foci observed in stage 14
791 oocytes (n = 40 and 52). Error bars represent standard deviation from the mean. **p =
792 0.0037, ***p = 0.0001, ****p<0.0001
793

794

795 **Figure 3**

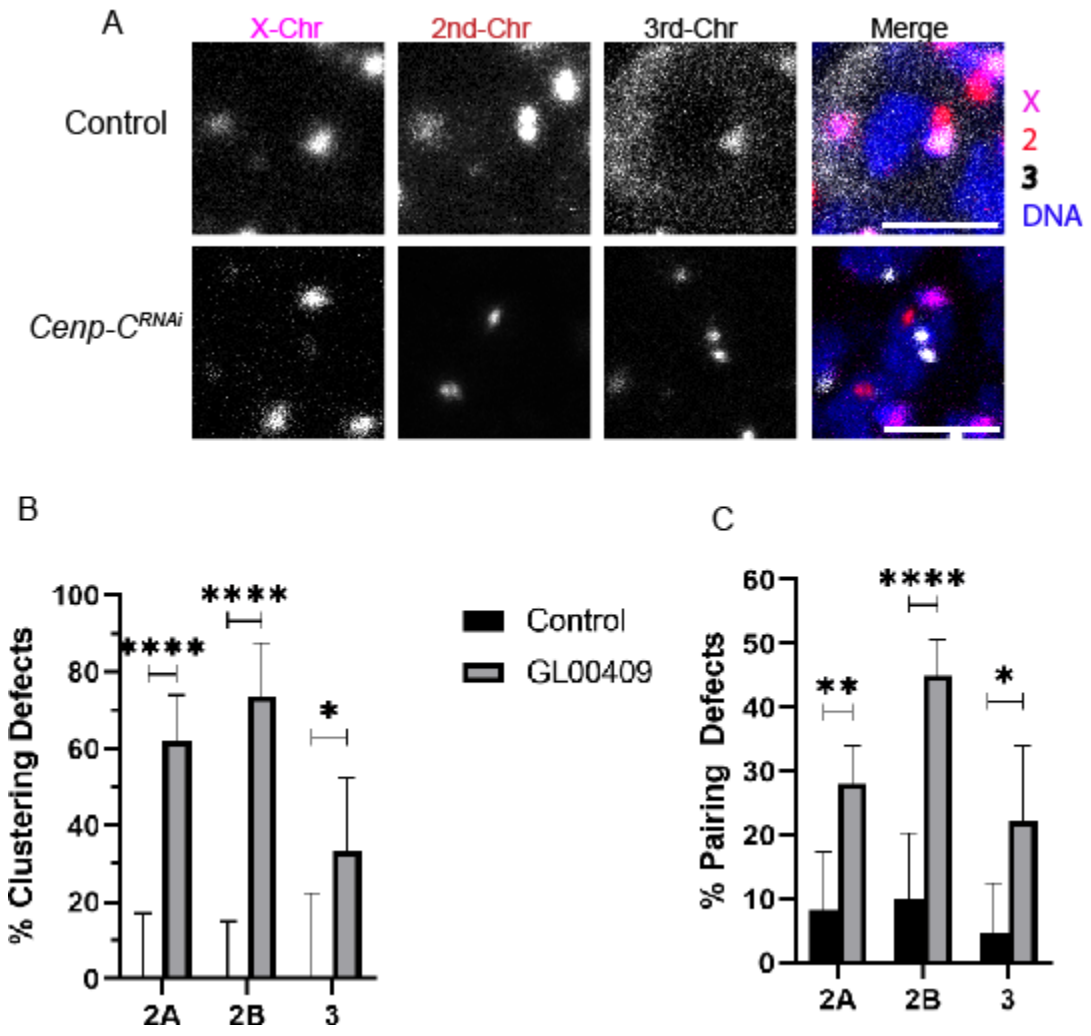

796

797 **Figure 3**

798 **CENP-C is required for centromere pairing and clustering. A)** FISH probes were
799 used to detect the pericentromeric regions of chromosome 2 (red), 3 (grey), and X
800 (magenta) in the germarium of *GL00409/NGTA* or control oocytes. DNA is in blue. **B)**
801 Clustering defects were defined as nuclei with greater than 2 of any centromere foci
802 (control n = 16, 20, 14; RNAi n = 42, 38, 18). **C)** Pairing defects were defined as oocytes
803 with greater than one focus for a chromosome in a nucleus. Scale bars represent 5mm.
804 * = 0.0196>p>0.0238, ** = 0.0045>p>0.0081, ****p<0.0001

805 **Figure 4**

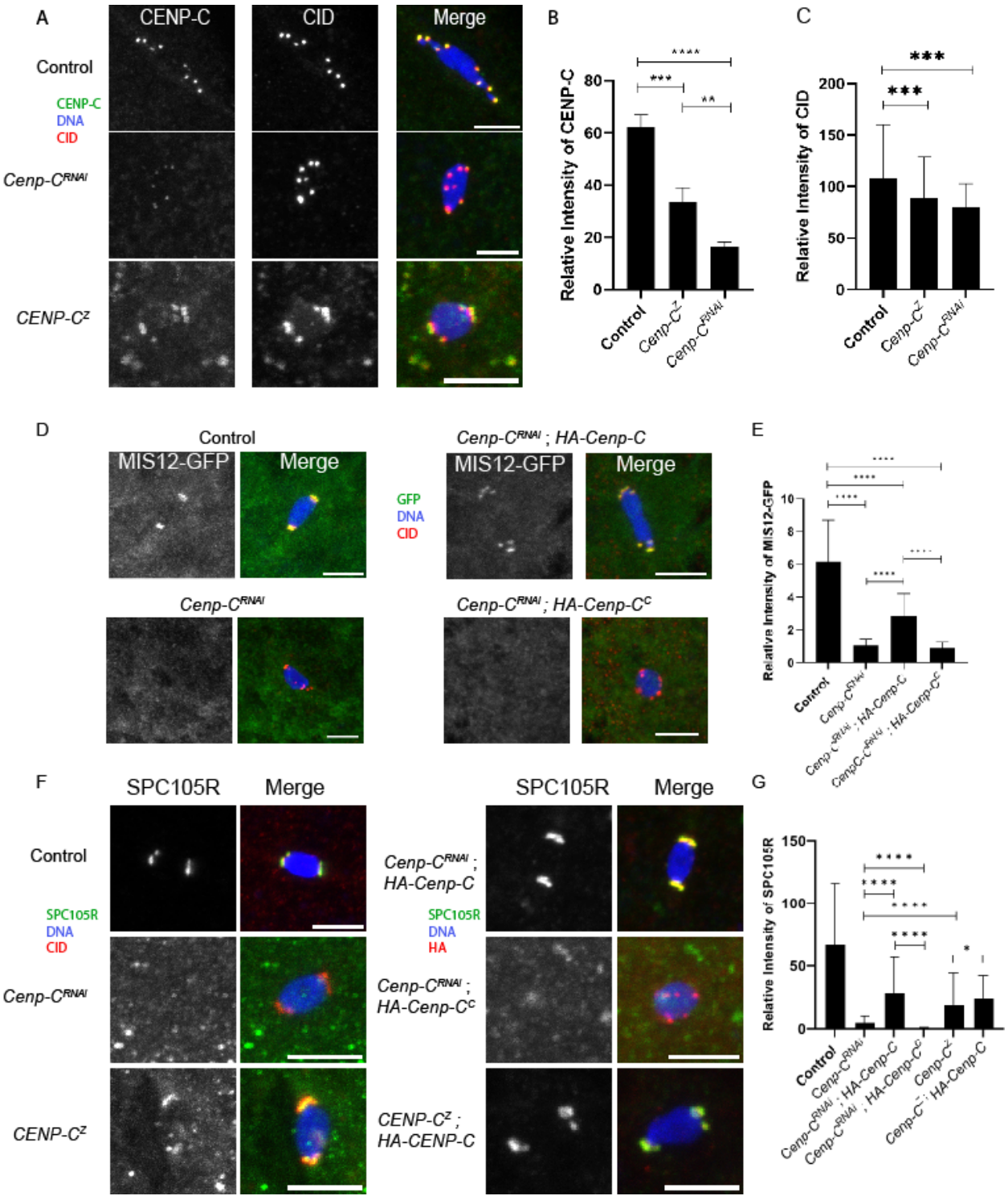

806

807

808

Figure 4

CENP-C is required for kinetochore assembly and chromosome segregation. Immunocytology was performed on stage 14 oocytes heterozygous for *Cenp-C* mutations (*Cenp-C*$^{Z3\text{-}4375}$/*Cenp-C*^{IR35} referred to as "*Cenp-C*^{Z}") or expressing the *GL00409* with *mata* (referred to as *Cenp-C*^{RNAi}). HA-tagged *Cenp-C* transgenes were coexpressed using the *mata* promoter in RNAi experiments or *osk-Gal4* in *Cenp-C*^{Z} experiments. **A)** Oocytes with CENP-C (green) and CID (red). **B)** The intensity of CENP-C was measured relative to background (n = 55, 67, 54). **C)** The intensity of CID was measured relative to background (n = 186, 221, 54). **D)** Oocytes expressing MIS12-GFP (green) and CID (red). **E)** Mis12-GFP localization was measured relative to the background (n = 57, 41, 47, 67). **F)** Oocytes with SPC105R (green) and CID (red). **G)** Intensity of SPC105R was measured relative to background (n = 108, 136, 115, 132, 245, 150). *p = 0.0379, **p = 0.0086, *** = 0.0002>p>0.0001, ****p<0.0001

825 **Figure 5**

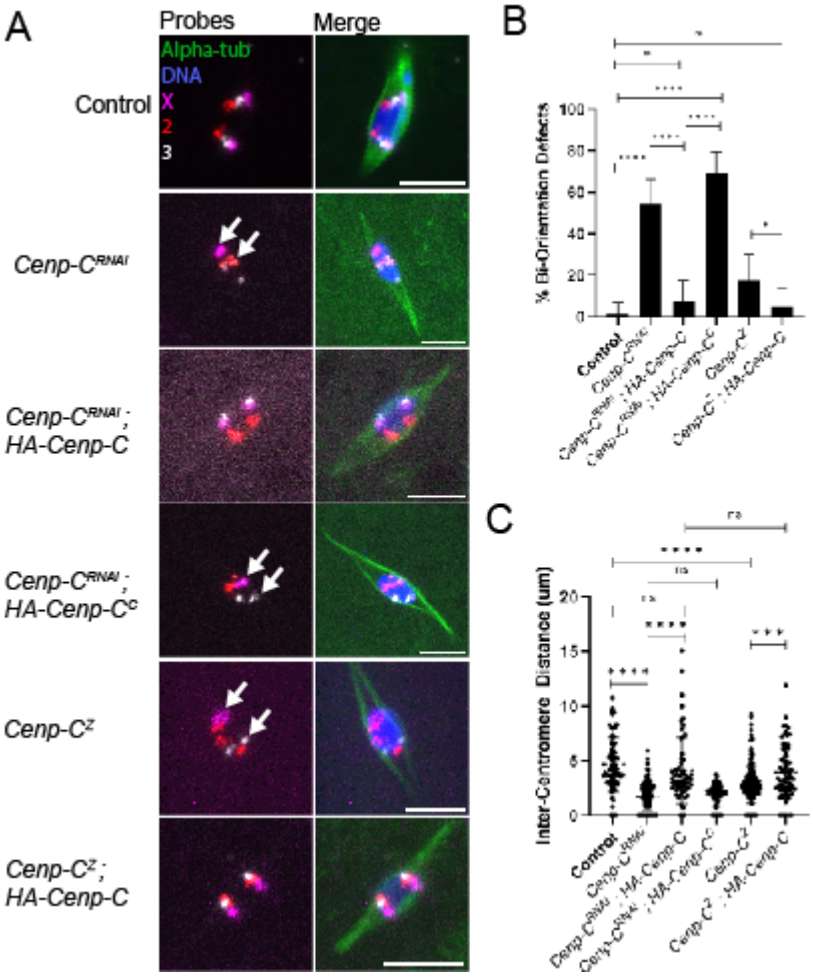

826

827 **Figure 5**

828 **Prophase-loaded CENP-C is required for bi-orientation in meiosis I. A)** FISH
829 probes were used to detect the pericentromeric regions of chromosome 2 (red), 3
830 (grey), and X (magenta). Stage 14 oocytes were *Cenp-C*$^{Z3\text{-}4375}$*/Cenp-C*^{IR35} (*Cenp-C*^{Z}) or
831 *GL00409/mata* (*Cenp-C*^{RNAi}), in some cases expressing *HA-Cenp-C* using *mata* in
832 *Cenp-C*^{RNAi} experiments or *oskGal4* in *Cenp-C*^{Z} experiments. **B)** Bi-orientation defects
833 were defined as two foci of the same probe that were on the same side of the spindle
834 midzone or only a single focus, indicating mono-orientation (n = 75, 59, 53, 58, 56, 60).
835 **C)** The distance between the center mass of two foci of the same probe was measured
836 as a readout for the microtubule tension across the kinetochore (n = 90, 156, 60, 60,
837 192, 72). All scale bars represent 5 mm and error bars represent standard deviation
838 from the mean. * = 0.0473>p>0.0387, **p = 0.0024, *** = 0.0002 >p> 0.001,
839 ****p<0.001.
840

841 **Figure 6**

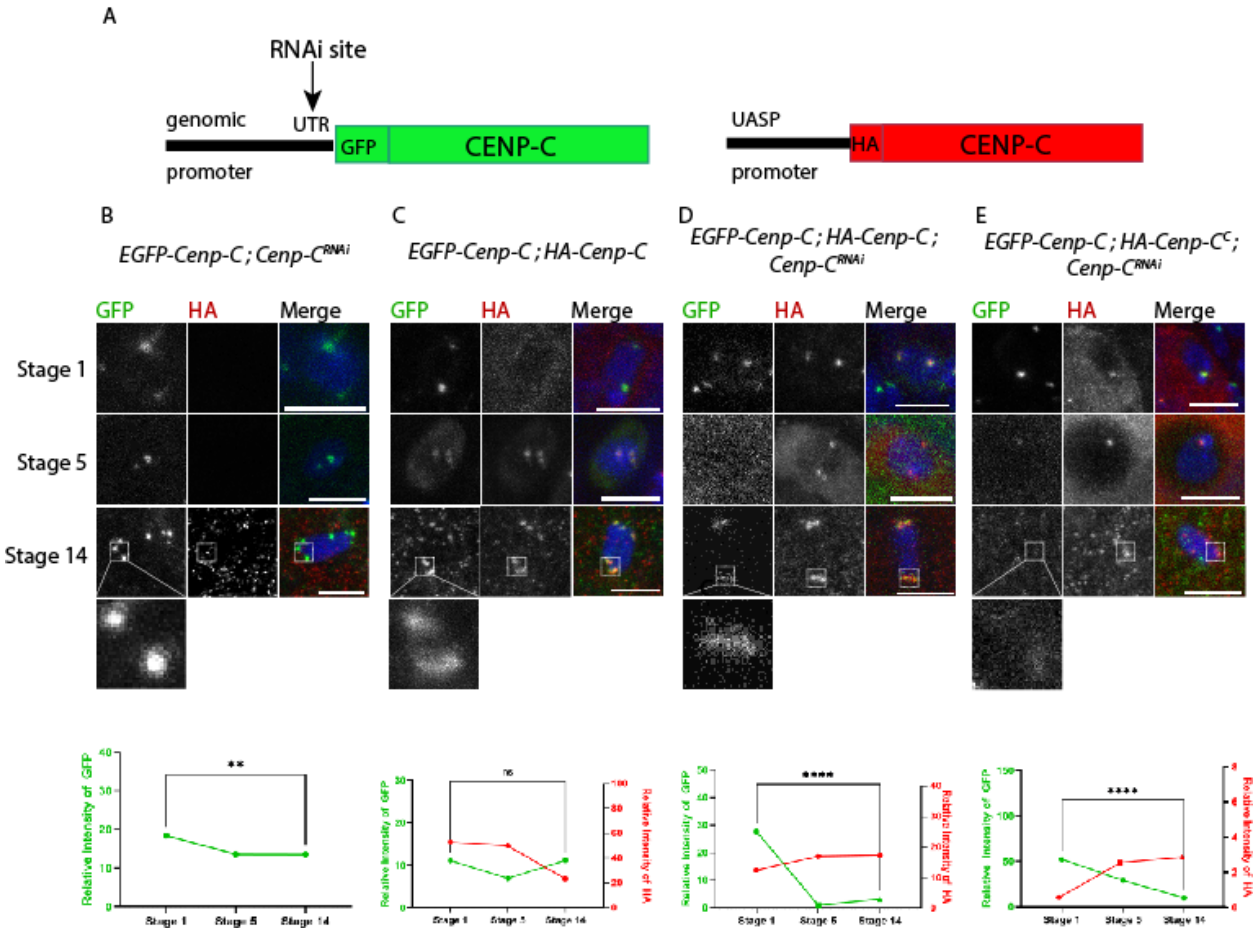

842

843 **Figure 6**

844 **CENP-C is exchanged at the centromeres during meiotic prophase. A)**
845 Immunocytology was performed on oocytes ubiquitously expressing GFP-CENP-C
846 (green), plus or minus *GL00409* (*Cenp-C*^{RNAi}) and HA-CENP-C (red), using the *mata*
847 promoter. *GL00409* recognizes a sequence in the 5' UTR, and, therefore, degrades
848 *GFP-Cenp-C* but not *HA-Cenp-C*. All scale bars represent 5 mm and DNA is blue. **B)**
849 With *GFP-Cenp-C* and *Cenp-C*^{RNAi} expression, the GFP levels decrease moderately
850 over time. **C)** With expression of *GFP-Cenp-C* and *HA-Cenp-C*, both GFP and HA foci
851 are observed. **D)** With expression of *GFP-Cenp-C*, *Cenp-C*^{RNAi}, and *HA-Cenp-C*, the
852 loss of GFP is associated with an increase in HA signal. **E)** Similar results were
853 observed with expression of *GFP-Cenp-C*, *Cenp-C*^{RNAi}, and *HA-Cenp-C*^{C}. Below each
854 image is a graph showing the relative centromeric intensity of GFP-CENP-C (green line)
855 and HA-CENP-C (red) for each genotype (n = 70, 23, 104; 117, 19, 156; 28, 19, 50; 67,
856 98, 90). For each genotype, the intensity between stage 1 and stage 14 was compared
857 using an unpaired t-test. ** p = 0.0016; ****p<0.0001.
858